Apoptosis (2015) 20:1457–1470
DOI 10.1007/s10495-015-1172-7

ORIGINAL PAPER

Apoptosis transcriptional mechanism of feline infectious peritonitis virus infected cells

Ahmad Naqib Shuid[1] · Nikoo Safi[1] · Amin Haghani[1] · Parvaneh Mehrbod[1,2] · Mohd Syamsul Reza Haron[1] · Sheau Wei Tan[1] · Abdul Rahman Omar[1,2]

Published online: 19 September 2015

Abstract Apoptosis has been postulated to play an important role during feline infectious peritonitis virus (FIPV) infection; however, its mechanism is not well characterized. This study is focused on apoptosis and transcriptional profiling of FIPV-infected cells following in vitro infection of CRFK cells with FIPV 79-1146 WSU. Flow cytometry was used to determine mode of cell death in first 42 h post infection (hpi). FIPV infected cells underwent early apoptosis at 9 hpi ($p < 0.05$) followed by late apoptosis at 12 hpi ($p < 0.05$) and necrosis from 24 hpi ($p < 0.05$). Then, next generation sequencing was performed on 9 hpi and control uninfected cells by Illumina analyzer. An aggregate of 4546 genes (2229 down-regulated and 2317 up-regulated) from 17 cellular process, 11 molecular functions and 130 possible biological pathways were affected by FIPV. 131 genes from apoptosis cluster (80 down-regulated and 51 up-regulated) along with increase of apoptosis, p53, p38 MAPK, VEGF and chemokines/cytokines signaling pathways were probably involved in apoptosis process. Six of the de-regulated genes expression (RASSF1, BATF2, MAGEB16, PDCD5, TNFα and TRAF2) and TNFα protein concentration were analyzed by RT-qPCR and ELISA, respectively, at different time-points. Up-regulations of both pro-apoptotic (i.e. PDCD5) and anti-apoptotic (i.e. TRAF2) were detected from first hpi and continuing to deregulate during apoptosis process in the infected cells.

Keywords Feline infectious peritonitis virus · Apoptosis · Transcriptome · Next generation sequencing · RT-qPCR · Flow cytometry

Introduction

Feline coronavirus (FCoV) is a spherical positive sense single-stranded RNA virus that is ubiquitous in wild and domestic *Felidae* family, with more than 90 percent prevalence in cats [1, 2]. The genome of this virus is approximately 30-kb in length with 11 open reading frames (ORFs) that encode 25 structural, non-structural and accessory proteins [3]. This virus has two main prototypes; feline enteric coronavirus (FECV) that usually causes subclinical or mild diarrhea with restricted infection in lower small intestine and colon [4] and feline infectious peritonitis virus (FIPV), which cause a systemic disease with granulomatous serositis with high amount of protein effusion (effusive FIP) or necrotizing and inflammatory lesions in variety of organs (non effusive FIP) [3]. Probably, FIPV is a virulent virus that arose from mutation in some sites like ORF 3c, spike (S) gene, and ORF 7b of FECV, which would change the enterocytes tropism to monocyte/macrophage cells [5]. These mutations would shift the localized intestinal infection to the severe systemic infectious peritonitis. Both these viruses contain two different serotypes based on virus neutralizing antibody reactions and sequencing [6]. Type I FCoVs are unique in cats with predominant prevalence in Europe and Americas [5]. Type II FCoVs with more than 25 % prevalence in

Electronic supplementary material The online version of this article (doi:10.1007/s10495-015-1172-7) contains supplementary material, which is available to authorized users.

✉ Abdul Rahman Omar
aro@upm.edu.my

[1] Institute of Bioscience, Universiti Putra Malaysia, 43400 Serdang, Selangor, Malaysia

[2] Faculty of Veterinary Medicine, Universiti Putra Malaysia, 43400 Serdang, Selangor, Malaysia

Asia is a double recombination of type I FCoVs and is closely related Canine CoV [7, 8].

Despite over 40 years of research, the mechanism of FIPV disease and induced immunity remains ambiguous. Severity of FIP is correlated with imbalance of B cells and T cells population, where the cell-mediated immunity can properly shift the disease to the dry form whilst, increase of B cells and antibody response can lead to type III hypersensitivity, antibody-dependent vasculitis and effusive form of the disease [6]. Hence, during FIPV infection, depletion of the lymphoid cells plays an important role in the virus pathogenesis [9]. In addition, infection of macrophages can increase B cells activity and contribute to antibody dependent enhancement (ADE) of the symptoms and effusive form of the disease [5]. Since FIPV does not infect lymphocytes, it seems that this virus cause the lymphopenia through apoptosis induction. Studies have reported that apoptosis of mononuclear cells and particularly CD8+ T cells in infected cats is associated with the secretion of TNF-alpha from macrophages [10]. On the other hand, decreased of TNF-α along with high amount of IFN-γ and IL-1β resulted in the augmentation of these CD8+ T-cells in peripheral blood mononuclear cells (PBMCs) of the infected cats [11]. Therefore, apoptosis T cell is probably caused by soluble mediators released from infection to macrophages and/or intestinal epithelial cells [10]. Further studies are required to elucidate the mechanism of apoptosis during FIPV infection. The current study is investigating mode of cell death of Crandell Rees feline kidney (CRFK) cells and the transcriptome of the infected cells following infection with FIPV WSU 79-1146. Furthermore, this study focused on understanding the apoptosis process during the infection and genes that may involve in apoptosis induction mechanism of the virus.

Materials and methods

Virus and cell line

Semi confluent 75 cm^3 tissue culture flasks of CRFK cells (ATCC® No: CCL-94™) were used for the time point infections. These cells were infected with 2 ml of FIPV WSU 79-1146 (ATCC® No. VR-2127™) with multiplicity of infection (MOI) of 3.0. After 1 h incubation for virus attachment, the infection media was replaced with 1 % FBS MEM and incubated at 37 °C with 5 % CO_2 depend on different time points of each phase of the study. Afterwards, cells were harvested using TrypLE™ and centrifuged twice in D-PBS at 4 °C for 10 min at 1000 rpm. Cell pellets were stored at −80 °C for further usages. The same process was repeated for the control group with the exception of 2 ml sterile D-PBS instead of the virus was used.

Apoptosis analysis

CRFK cells were infected with FIPV strain WSU 79-1146 (ATCC® No: VR-2127™) (MOI of 3.0) at different time points (0, 3, 6, 9, 12, 15, 18, 21, 24, 27, 30, 33, 36, 39 and 42 h) to determine the mode of cell death during virus infection. FIPV-infected CRFK cells were incubated with FITC-labeled Annexin V and harvested using TrypLE™ Express. Detection of early apoptosis, late apoptosis and necrosis was carried out by using flow cytometer (Becton–Dickinson FACScalibur Flow Cytometer) and the readings for each group of samples (in triplicates) at each time points were then calculated using BD CellQuest software (BD Bioscience, USA). The analyses were performed using 10,000 cells stained with Annexin V-FITC/PI. The mean and standard deviation for samples at each time point were calculated and paired t test (two-tailed) was conducted between control and treated cells at 0.05 level of significance in different time points using SPSS statistical software version 22 (SPSS Inc., Chicago, IL, USA).

Transcriptomic studies

RNA extraction

For sequencing, the samples from control and infected cells that started to undergo significant early apoptosis at 9 hpi was chosen for RNA extraction and further analysis. RNeasy® Mini Kit (Qiagen®, USA) was used to extract and purify RNA samples following the method recommended by the manufacturer. The quality of the extracted RNA was determined by Ultrospec 3000 Pro UV/Visible spectrophotometer (GE Healthcare, UK), where samples with an absorbance ratio value (A260/A280) of 1.8–2.0 were considered for further analysis with Agilent® 2100 Bioanalyzer. Samples with RNA integrity numbers (RIN) 9–10 and concentrations higher than 500 ng/μl per sample, were sent for next generation sequencing analysis using Illumina GAII Analyzer.

RNA sequencing and bioinformatics analysis

RNA sequencing was performed on control and 9 h infected CRFK cells with FIPV WSU 79-1146. Filtered raw data was then mapped separately to GTF format annotated 2× whole genome shotgun sequencing of *Felis catus* downloaded from www.ensembl.org (PubMed ID 17975172) reference using CLC bio Genome Workbench (GWB) RNAseq function with minimum length fraction of 0.9, maximum mismatches of two and maximum number

of hits for a read of ten (CLC bio version 4.7.0, Aarhus, Denmark). An aggregate of 20 GB of the sequencing data which included both control and infected samples, was imported into the CLC bio GWB (CLC bio version 4.7.0, Aarhus, Denmark). The sequences were trimmed for adapter sequences and low quality base. The trimmed raw sequences were subjected to RNA-sequence analysis, by mapping them to an annotated feline genome reference sequence accounting for a maximum of two gaps or mismatches in each sequence. The relative transcript levels were considered as output and expressed as reads per kilobase of exon model per million mapped reads (RPKM) [12]. Significant differentially expressed genes were selected via Kal's Z test on proportional differences and FDR value less than 0.05 (FDR < 0.05) and fold change >1.99. Later, the genes were converted into Unigene IDs format for further functionally annotated analysis in Panther database. The resulting list was then converted from Ensembl transcript ID to EntrezGene ID using Ensembl Genes 73 database (*Felis_catus*_6.2 data sets) at Biomart (http://www.ensembl.org). Then, gene ontology of PANTHER database was applied for interpretation of biological processes, molecular function, and pathways of genes with significant deregulation level in FIPV-infected CRFK cells compared to control, (http://www.pantherdb.org) (Applied Biosystem) [13].

Real time qPCR analysis

Based on bioinformatics analysis, five deregulated genes of the apoptosis cluster were chosen for further analysis; namely, Ras association (RalGDS/AF-6) domain family member 1 (RASSF1), Basic Leucine Zipper Transcriptional Factor ATF-Like 2 (BATF2), Melanoma antigen family B 16 (MAGEB16), Programmed cell death 5 (PDCD5) and TNF receptor-associated factor 2 (TRAF2). RNA samples from CRFK cells infected with FIPV strain WSU 79-1146 (ATCC® No: VR-2127™) (MOI of 3.0) at different time points (0, 1, 3, 9, 24 and 48 hpi) were extracted as described above followed by cDNA synthesis (High-Capacity cDNA Reverse Transcription Kit, Applied Biosystems®). Four µl of each cDNA was used to perform real-time qPCR using Maxima SYBR Green qPCR master mix (Thermo Scientific, USA) and specific primers for each gene (Table 1). Melting curve analysis was performed to confirm the specificity of the results. In addition, for all these genes, non-template controls (NTC) were run in parallel with the samples. The mean C_t values of all genes were normalized with three housekeeping genes (GAPDH, ACTB2 and GUSB) for relative expression analysis. Analysis of variance (ANOVA) followed by Post Hoc Tukey HSD was conducted to determine the differences among the time points at 0.05 level of significance.

Analysis of TNFα mRNA and protein concentration in FIPV infected cells

Previous studies have indicated the involvement of TNFα in inducing apoptosis during FIPV infection [14], hence, we analysed both the mRNA and the intracellular as well as the extracellular protein concentration of TNFα during first 48 h post infection. For each time points (0, 3, 9, 24 and 48 hpi), three CRFK semi confluent 25 mm^2 flasks were infected with FIPV strain WSU 79-1146 (ATCC® No: VR-2127™) as described before. Afterwards, the cells and supernatant of the flasks were collected at the targeted time points. The expression of TNFα was evaluated by RT-qPCR as described in previous section. For intracellular proteins, the cells were lysed in 700 µl of cytobuster™ protein extraction reagent (Novagen, USA) with 2 % protease inhibitor cocktail from Protein extraction kit (ab65400) (Abcam, UK). Then, the protein concentrations were evaluated by photospectrometer (Eppendorf, Germany) and all the concentrations were normalized prior to analysis. For extracellular protein analysis, the supernatants were concentrated for 50 % using a centrifugal vacuum concentrator (Eppendorf, Germany) prior to analysis. Subsequently, the protein concentrations were analysed by enzyme linked immunosorbent assay (ELISA) kit specific for TNFα detection (Catalog no. CATA00; R&D systems, USA) according to manufacturer instruction.

Results

CRFK cells infected with FIPV undergo early apoptosis with significant decreased in the number of viable cells at 9 hpi ($p < 0.05$). The number of cells that underwent early apoptosis increased from 363.33 ± 27.17 cells ($p < 0.01$) at 9 hpi to 3824.33 ± 14.11 cells ($p < 0.001$) at 42 hpi. Similar pattern was observed in late apoptotic cells as well, where the number of late apoptotic cells increased significantly at 12 hpi with 477.67 ± 82.56 cells ($p < 0.05$) and increased further to 3815.33 ± 97.90 cells ($p < 0.001$) at 42 hpi. The number of cells that underwent necrosis started to increase significantly ($p < 0.05$) only at 24 hpi (Figs. 1 and 2; Table 2). Hence, this study showed that FIPV efficiently destroyed infected cells by inducing apoptosis as early as 9 hpi followed by necrosis after 24 hpi.

Total RNA from the control and 9 hpi samples were sequenced using Illuminia GAII sequencer. From the raw sequences obtained in a form of 20 GB fastq format data, low-quality reads were filtered out at high stringency which produced 52.54 % (50,467,524) of control and 47.46 % (45,593,004) of infected samples of high-quality 100 bp sequence length (data not shown). The distribution of

Table 1 Primer sequences of apoptotic related genes and housekeeping genes used for RT-qPCR study

Genes	Primers sequence	Role in apoptosis
Basic leucine zipper transcriptional factor ATF-like 2 (BATF2)	5′-TGAAGGAGCAGCCATAGC-3′	Pro apoptosis
	5′-ACATAAGGTAATAGCGGTGACA-3′	
Ras association domain-containing protein 1 (RASSF1)	5′-CTGGAGGCGTGGCGTGTAT-3′	Pro apoptosis
	5′-GACGGCTAGGATCTGGCTCTTG-3′	
TNF receptor-associated factor 2 (TRAF2)	5′-CCGCTACTGCTCCTACTG-3′	Anti apoptotic
	5′-AAATGCCCTCTTCGTATATGC-3′	
Programmed cell death protein 5 (PDCD5)	5′-GAAACAGTATCTTAGCCCAAGTC-3′	Pro apoptotic
	5′-CCACTTAGTTGCCCGTATCT-3′	
Melanoma-associated antigen B16 (MAGEB16)	5′-GCCAGATGCCAAGAATGTG-3′	Pro apoptotic
	5′-AGCGAAGTGCTCTTCATACC-3′	
Tumor necrosis factor alpha (TNFα)	5′ -ATCAATCTGCCTAACTATCT-3′	Pro apoptotic
	5′ -CTGAGCCCTTAATTCTCT-3′	
Glyceraldehyde 3-phosphate dehydrogenase (GAPDH)	5′-GCTGAGTATGTTGTGGAGTC-3′	House keeping gene
	5′-GCAGAAGGAGCAGAGATGA-3′	
Glucuronidase β (GUSB)	5′-AACTCCAACTATGAAGCAGACCT-3′	House keeping gene
	5′-TGCTCCGTACTCGCTCTG-3′	
Actin, beta-like 2 (ACTBL2)	5′-CAGGAGTACGACGAGTCCG-3′	House keeping gene
	5′-CAAGAAAGGGTGTAACGCAACT-3′	

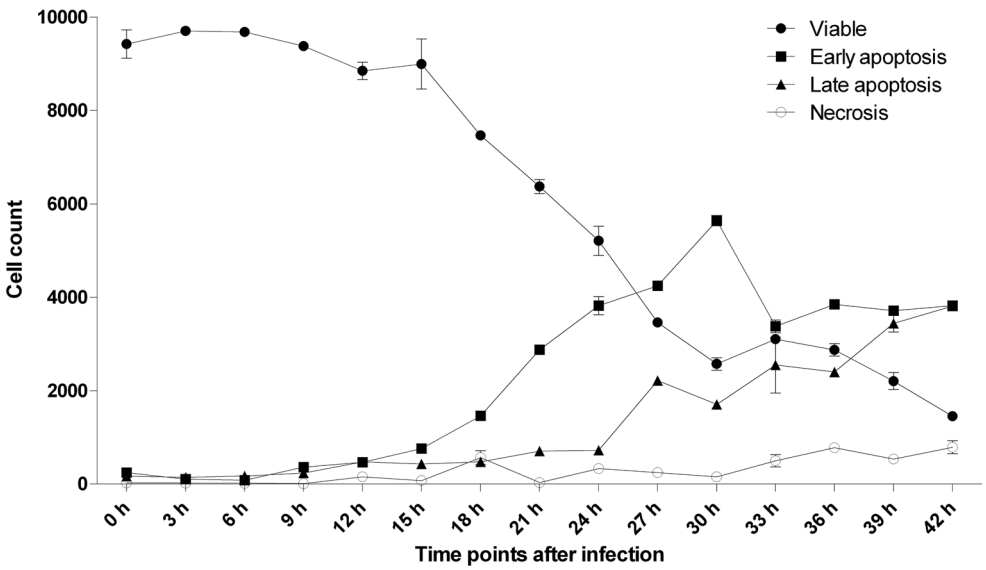

Fig. 1 Trend of viable cell depletion, early apoptosis, late apoptosis and necrosis of CRFK cells infected with FIPV

original expression values were found to be positively skewed for both control and infected samples where the median (M) value is higher in control (M = 1) compared to the infected sample (M = 0) (Fig. 3). Hence, the original expression values were normalized. The normalized expression values also resulted in positive skewed distribution in both control and infected samples. There were no outliers observed and both the control and infected samples possessed the same median (M = 1). The IQR for both samples was 10 and the range for both samples was also 10 (Fig. 3). As a result of normalization, both samples, on average possessed similar expression values and variability. The normalized expression value data were used for subsequent analysis using CLC bio Genomic Workbench for the identification of deregulated genes involved in cell cycle, apoptosis and immune responses.

Panther's gene analysis revealed that a total of 4546 (2229 down-regulated and 2317 up-regulated) with fold

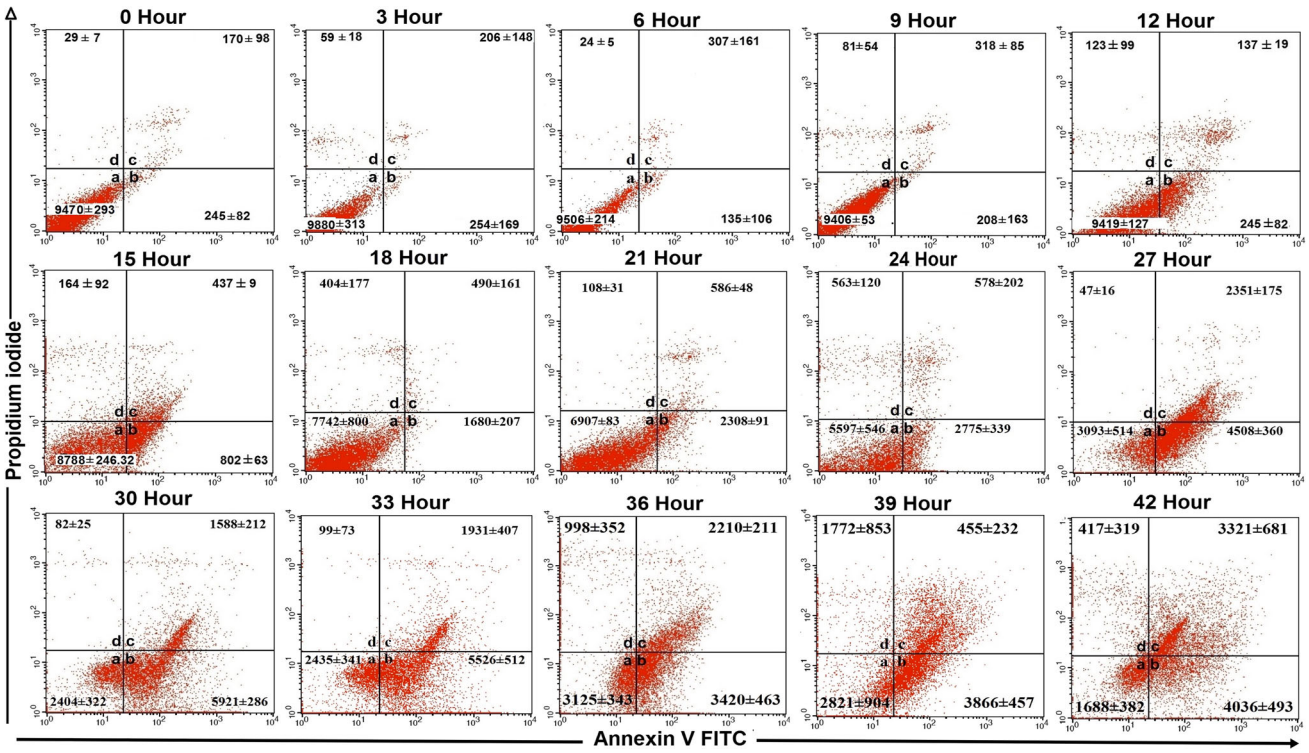

Fig. 2 Flow cytometer analysis of FIPV infected CRFK cells from 0 to 42 h of infection. Regions inside the graphs include: **a** non-apoptotic cells (Annexin V-FITC$^-$/PI$^-$). **b** Early apoptotic cells (Annexin V-FITC$^+$/PI$^-$). **c** Late apoptosis/necrotic cells (Annexin V-FITC$^+$/PI$^+$). **d** Dead cells (Annexin V-FITC$^-$/PI$^+$)

change more than 2 ($X > 2$) and less than -2 ($X < -2$) with FDR <0.05 were deregulated at 9 hpi. Furthermore, gene ontology (GO) analysis based on Panther database could analyze 2528 of these deregulated genes based on cellular processes, molecular functions and involved pathways. These genes were accounted for 4854 cellular processes involved in 17 cellular such as apoptosis, immune system and metabolic processes, whilst based on molecular functions, these genes were related to 2854 functions divided into 11 clusters, which mostly related to catalytic and binding activities. Tables 3 and 4 show the clusters of the affected genes by FIPV at 9 hpi according to different cellular processes and molecular functions, respectively. Panther pathway analysis revealed that 1096 of these genes belonged to 130 possible cellular pathways, which can be affected by FIPV at 9 hpi of the CRFK cells. Some of the most affected pathways include Wnt signaling, inflammation mediated by chemokines and cytokines signaling, integrin signaling and apoptosis signaling pathways. The pathways containing more than 10 deregulated genes are listed in Table 5. Among the resulted clusters, 131 genes were classified as apoptosis genes (80 down-regulated and 51 up-regulated genes) with absolute fold change more than 2 and FDR <0.05. In addition, 25 genes were detected from the apoptosis-signaling pathway. A total of 14 most significant down and up regulated genes from the apoptosis cluster after FIPV infection are shown in Tables 6 and 7.

In the apoptosis-signaling pathway, 25 genes were significantly deregulated (FDR <0.05, PFC >2 or <−2) (Table 8). Some of the important effects of FIPV on this pathway include activation of tumor necrosis factor ligand and Fas mediated apoptosis through up regulation of TNF receptor associated death domain (TRADD), Fas associated death domain (FADD) and death associated protein 6 (DAXX). In addition, several of the anti apoptotic genes like protein kinases genes (PRKCD, AKT3, and PRKCA) were down regulated. This pathway also showed some anti apoptotic signaling like up regulation of TRAF2 and nuclear factor Kappa-B (NFKB2) and down regulation of Caspase 7 (CASP7) genes.

Five up regulated pro apoptotic genes (RASSF1, BATF2, MAGEB16, PDCD5, TNFα) and one up regulated anti apoptotic gene (TRAF2) were selected from apoptotic cluster for further validation via RT-qPCR. In qPCR, the trend of expression changes was investigated in first 48 hpi following infection with FIPV. All these genes showed up-regulation trend during this period, which is in accord with the transcriptomic study (Fig. 4).

Table 2 Flow cytometry analysis of Annexin V-FITC staining of control and infected CRFK cells at different time points with significant difference levels: $p < 0.05$ marked with *, $p < 0.01$ marked with ** and $p < 0.001$ marked with ***)

Time (h)	Sample	Viable			Early apoptosis			Late apoptosis			Necrosis		
		Mean (n = 3)	±SD	p value	Mean (n = 3)	±SD	p value	Mean (n = 3)	±SD	p value	Mean (n = 3)	±SD	p value
0	Control	9468.60	292.66	0.696	181.40	123.50	0.696	234.00	166.44	0.119	25.00	3.67	0.792
	Sample	9426.20	301.92		244.80	82.15		170.00	97.92		29.00	7.00	
3	Control	9814.00	73.51	0.119	84.67	24.83	0.398	124.00	20.52	0.163	26.00	6.00	0.915
	Infected	9702.00	34.04		108.00	19.35		147.33	12.50		26.67	3.79	
6	Control	9677.00	16.52	0.584	79.33	14.72	0.853	195.00	42.57	0.481	21.17	2.84	0.912
	Infected	9682.33	30.17		83.33	4.48		172.33	15.31		20.00	17.35	
9	Control	9723.83	31.76	0.012*	73.67	4.63	0.007**	180.67	26.50	0.122	16.67	1.53	0.230
	Infected	9383.00	56.51		363.33	27.17		237.33	21.08		10.33	6.66	
12	Control	9824.00	59.03	0.013*	128.33	17.13	0.030*	114.00	9.00	0.015*	151.00	21.07	0.765
	Infected	8852.00	183.67		469.33	48.26		477.67	82.56		157.67	33.47	
15	Control	9491.33	57.35	0.256	357.67	15.17	0.002**	200.00	42.32	0.008**	63.00	27.78	0.499
	Infected	8998.00	536.68		762.67	18.35		431.67	6.66		76.33	1.53	
18	Control	9255.00	52.37	0.002**	134.00	32.42	0.010*	311.33	23.97	0.064	117.00	9.64	0.035
	Infected	7466.67	80.60		1465.00	103.10		478.67	52.88		567.00	149.28	
21	Control	9410.00	112.30	0.000***	170.00	14.53	0.001**	202.67	84.20	0.004 **	22.67	1.53	0.155
	Infected	6375.67	148.43		2876.00	67.49		707.33	28.99		32.33	6.03	
24	Control	9704.00	27.22	0.002**	0.00	0.00	0.003**	97.33	8.08	0.001**	218.67	7.37	0.067*
	Infected	5208.67	312.30		3824.67	195.70		725.67	20.98		332.67	53.14	
27	Control	9650.33	155.36	0.000***	45.67	4.67	0.000***	6.33	5.86	0.000***	58.33	2.08	0.007**
	Infected	3463.33	25.42		4252.67	28.22		2223.67	24.68		246.00	24.76	
30	Control	9289.67	80.90	0.000***	119.33	30.67	0.001**	391.67	55.59	0.001**	75.33	3.79	0.007**
	Infected	2573.67	134.44		5642.67	112.69		1707.67	86.56		155.67	12.42	
33	Control	9150.33	47.12	0.000***	132.33	8.09	0.002**	478.67	36.86	0.024*	315.33	13.01	0.133*
	Infected	3103.67	82.50		3383.00	135.88		2550.67	596.44		501.00	130.09	
36	Control	9443.00	93.50	0.000***	365.00	26.54	0.000***	80.00	50.39	0.000***	471.33	18.50	0.024*
	Infected	2873.67	133.59		3851.33	78.19		2403.00	78.79		783.00	89.45	
39	Control	8874.67	212.43	0.000***	384.67	42.18	0.001**	127.67	15.31	0.001**	307.33	17.04	0.019*
	Infected	2209.67	178.16		3716.33	61.06		3446.00	187.98		538.33	73.28	
42	Control	9176.67	129.77	0.000***	247.00	7.94	0.000***	142.00	30.61	0.000***	460.33	25.38	0.039*
	Infected	1455.33	46.72		3824.33	14.11		3815.33	97.90		792.00	137.71	

SD standard deviation, *n* number of samples

Among the pro apoptotic genes, significant change in expression of BATF2 was detected at 9 hpi and this trend continued during until 48 hpi (Fig. 4). It is worth mentioning that BATF2 was the only gene that showed significant up regulation at 48 hpi time point. The expression of all the other genes started to down regulated after 24 hpi (Fig. 4). On the other hand, PDCD5 expression started to increase at 1 hpi with an ascending trend until 24 hpi. Afterwards, the expression level decreased gradually until a significant ($p < 0.05$) down regulation compared to the control cells at 48 hpi. Another targeted pro apoptotic gene of this study is RASSF1. This gene did not increased at first 3 hpi. However, after this time point, the expression level commenced to augment gradually and remained up regulated at 9 and 24 hpi. However, the expression of this gene decreased to the normal state at 48 hpi. As opposed to the previous genes, MAGEB16 remained normal at first 9 hpi (Fig. 4). This gene was the only gene that did not show significant up regulation ($p < 0.05$) during this period. Subsequently, the expression of MAGEB16 significantly increased at 24 hpi and once more decreased to the normal state at 48 hpi.

With regards to gene with anti-apoptotic function, significant increased of TRAF2 was detected from the first hour of infection. This level of expression remained high until 24 hpi. Subsequently, the expression gradually reduced to the normal state at 48 hpi (Fig. 4). Relative

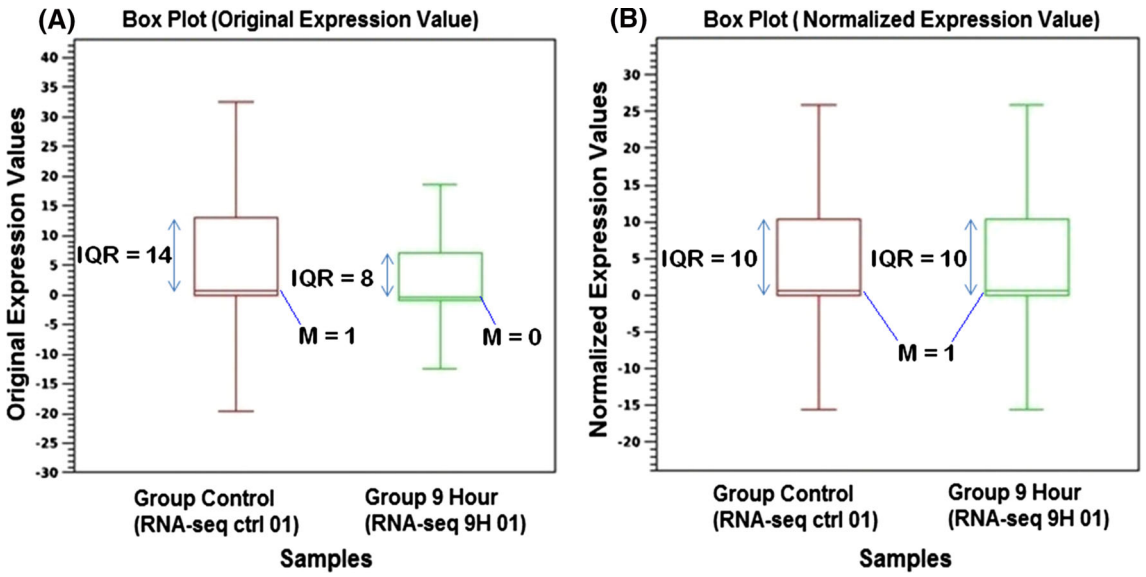

Fig. 3 Box plot analysis between original expression values and normalized expression values by using CLC bio Genomic Workbench statistical analysis

Table 3 Clustering of the deregulated genes in FIPV infected CRFK cells according to biological processes

Biological processes	No of genes		
	Total	Up-regulated	Down regulated
Cell communication (GO:0007154)	461	177	284
Cellular process (GO:0009987)	754	307	447
Localization (GO:0051179)	29	10	19
Transport (GO:0006810)	389	139	250
Cellular component organization (GO:0016043)	186	69	117
Apoptosis (GO:0006915)	131	51	80
System process (GO:0003008)	210	73	137
Reproduction (GO:0000003)	96	46	50
Response to stimulus (GO:0050896)	201	101	100
Regulation of biological process (GO:0050789)	6	3	3
Homeostatic process (GO:0042592)	15	6	9
Developmental process (GO:0032502)	345	138	207
Generation of precursor metabolites and energy (GO:0006091)	58	30	28
Metabolic process (GO:0008152)	1261	618	643
Cell cycle (GO:0007049)	268	113	155
Immune system process (GO:0002376)	289	138	151
Cell adhesion (GO:0007155)	155	51	104

expression analysis of these selected genes by RT-qPCR was in accord with results of the NGS fold change analysis. The only gene that did not show significant up regulation at 9 hpi was MAGEB16, which started to increase at 24 hpi.

Although TNFα did not show significant deregulation at 9 hpi using RNA-seq analysis, the number of related affected genes including significant up regulation of FADD, TRADD, TRAF2, Tumor necrosis factor induced protein 1 and 3 (TNFAIP1 and TNFAIP3) show the importance of analysis of this cytokine during apoptosis mechanism of FIPV. Since specific feline TNFα antibody is not available commercially, the kit for canine TNFα detection, which has high homology to feline, was used during this analysis. Both RT-qPCR and ELISA analysis showed that TNFα production would be significantly increased during first 48 hpi of FIPV. The production of this cytokine started to increase significantly ($p < 0.05$) at 3 hpi compared to negative control. At 9 hpi, although

Table 4 Clustering of the deregulated genes in FIPV infected CRFK cells according to molecular function

Molecular functions	Deregulated genes		
	Total	Up-regulated	Down regulated
Ion channel activity (GO:0005216)	28	9	19
Transporter activity (GO:0005215)	150	49	101
Translation regulator activity (GO:0045182)	31	11	20
Transcription regulator activity (GO:0030528)	221	141	80
Enzyme regulator activity (GO:0030234)	152	62	90
Catalytic activity (GO:0003824)	892	389	503
Motor activity (GO:0003774)	22	0	22
Receptor activity (GO:0004872)	169	62	107
Antioxidant activity (GO:0016209)	8	4	4
Structural molecule activity (GO:0005198)	253	116	137
Binding (GO:0005488)	928	483	445

neither mRNA expression level and intracellular concentration of TNFα did not show any significant difference with control, the extracellular concentration of this cytokine still showed significant higher concentration compared to uninfected cells; which probably explain the up regulation in other related genes at this time point. At 24 hpi, both intracellular and extracellular TNFα concentration started to drop to the normal state, which was in contrast to expression level of this gene that started to significantly increase at this time point. Subsequently, TNFα started to significantly increase in expression and both intracellular and extracellular protein concentration until 48 hpi of FIPV (Fig. 5).

Discussion

Studies have showed that FIPV can be classified into 2 serotypes, serotype I are difficult to growth in cell culture compared to serotype 2 namely WSU 79-1146, etc. [15]. Previous studies have shown that cytopathic effects (CPE) of FIPV infected CRFK cells can be observed between 42 and 50 h of infection [16, 17]. However, the cell death mode of the infected cells is not characterized. In this study, we characterized FIPV infected cells based on flow cytometry measurement along with transcriptome analysis of genes that were deregulated in the infected cells. In addition to FIPV, CRFK cells have been used to study apoptosis of other feline viruses such as feline immunodeficiency virus (FIV) and feline calcivirus (FCV). Previous studies have shown that FIV can induce apoptosis in CRFK cells through TNF-α signalling, caspase activation and NF-κB pathways [14, 18], whilst, FCV also induce apoptosis of CRFK cells via mitochondrial pathways and activation of an executioner caspase like caspase 3 [19]. Hence, CRFK cells can be a suitable in vitro model for studying the apoptosis process of FIPV infected cells.

The mechanism of apoptosis induction in lymphoid tissue of FIPV-infected cats remains unclear although lymphocyte depletion and the presence of apoptotic cells were found in the T-cell region of mesenteric lymph nodes and spleen of cats with FIP [20, 21]. However, since FIPV does not replicate in peripheral blood lymphocytes, it is difficult to consider that lymphopenia is due to direct destruction by virus infection of lymphocytes. We hypothesized that FIPV infected cells might release mediators that cause the induction of apoptosis of lymphocytes. Study has shown that TNF-α released from macrophages of FIP cats, induced apoptosis in lymphocytes, particularly CD8+ T cells [10]. Transcriptome analysis of FIPV infected cells showed that the virus probably increase the inflammation through the chemokine and cytokine signaling pathways, Wnt signaling, Cadherin signaling, to name but a few (Tables 3, 4, 5). After 9 hpi, this virus could significant deregulate 4526 genes, which is much higher than 96 genes at 3 hpi according to a previous study by Harun et al. [22]. In addition, the expression of some of the ISG genes (e.g. ISG15 and ISG20), pro inflammatory and Th1-like cytokines (e.g. CCL8, CXCL10, and CCL17), genes related to innate immune responses (e.g. PHF11 and IRF1), and some genes like MX1 also showed significant up regulation (Supplementary Table 1), confirming the findings from previous study by Harun and his colleagues [22].

The current results also showed that the virus would efficiently induce apoptosis at 9 hpi by increasing the apoptosis signaling pathways and many other factors like p53 pathway, vascular epithelial growth factor (VEGF) signaling, p38 signaling for over production of cytokines and chemokines/cytokines receptors (Table 5). A previous study has indeed indicated that VEGF is highly related to

Table 5 Pathways with more than 10 deregulated genes (FDR <0.05) after infection of CRFK cells with FIPV

Pathways	No of genes
Wnt signaling pathway (P00057)	50
Integrin signalling pathway (P00034)	46
Gonadotropin releasing hormone receptor pathway (P06664)	44
Inflammation mediated by chemokine and cytokine signaling pathway (P00031)	42
Huntington disease (P00029)	35
EGF receptor signaling pathway (P00018)	35
Angiogenesis (P00005)	34
FGF signaling pathway (P00021)	32
p53 pathway (P00059)	27
Alzheimer disease-presenilin pathway (P00004)	26
Apoptosis signaling pathway (P00006)	25
Parkinson disease (P00049)	25
Cytoskeletal regulation by Rho GTPase (P00016)	25
PDGF signaling pathway (P00047)	23
TGF-beta signaling pathway (P00052)	22
Cadherin signaling pathway (P00012)	22
Ras pathway (P04393)	19
Toll receptor signaling pathway (P00054)	18
B cell activation (P00010)	18
Endothelin signaling pathway (P00019)	17
T cell activation (P00053)	16
Nicotinic acetylcholine receptor signaling pathway (P00044)	16
Ubiquitin proteasome pathway (P00060)	15
Heterotrimeric G-protein signaling pathway-Gi alpha and Gs alpha mediated pathway (P00026)	15
Alzheimer disease-amyloid secretase pathway (P00003)	14
VEGF signaling pathway (P00056)	14
Transcription regulation by bZIP transcription factor (P00055)	14
Interleukin signaling pathway (P00036)	14
p38 MAPK pathway (P05918)	14
Heterotrimeric G-protein signaling pathway-Gq alpha and Go alpha mediated pathway (P00027)	12
Angiotensin II-stimulated signaling through G proteins and beta-arrestin (P05911)	11
DNA replication (P00017)	11
p53 pathway feedback loops 2 (P04398)	10

pyogranuloma and effusive form of the disease [23]. The importance of p38 mitogen-activated kinase (MAPK) pathway in cytokines production also has been reported by Regan et al. [24] during FIPV infection. A study showed that medium from FIPV infected macrophage-derived (fcwf-4) cell line could not induce apoptosis to cultured T cells [20] proposing that mediators released from virus infection to epithelial cells may cause T cells death and depletion. This can explain the reason of chemokines and cytokines signaling augmentation in parallel with increase of apoptosis during the infection (Table 5). Furthermore, it has been reported that apoptosis prompt the activation of endogenous endonucleases, which lead to fragmentation of cellular DNA [20]. Hence, FIPV might use apoptosis as a viral strategy to enhance the spread of progeny to neighboring cells.

Previous studies have highlighted that the augmentation of TNF-α production by FIPV and the possible role of adipokine in apoptosis induction and depletion of CD8+ T cells [10]. The results of this study also revealed that this virus would increase the production of this cytokine during first 48 hpi, which would activate TNF receptor superfamily (TNFR and Fas) signaling and cause overexpression of TRADD and FADD associated with the activation of these mechanisms after FIPV infection (Table 8). Previous studies have indeed showed that TRADD up regulation can

Table 6 List of down-regulated genes from apoptosis cluster

	Genes	PFC	Accession no.	Function
1	ADAMDEC1	−104.59	XM_845854	Control immune response during pregnancy
2	NEO1	−96.30	AC012670	May act as regulatory protein in the transition of undifferentiated proliferating cells to their differentiated state
3	YES1	−86.61	AC192398	Regulating cell growth and survival, apoptosis, cell–cell adhesion, cytoskeleton remodeling and differentiation
4	ADAM19	−66.98	AC008694	Participates in the proteolytic processing of beta type neuregulin isoforms
5	TMEM47	−47.52	NM_138751	Localized to the endoplasmic reticulum and in the plasma membrane
6	API5	−32.19	NM_001127379	Prevents apoptosis after growth factor deprivation
7	DAPK1	−27.57	AC235013	Positive mediator of gamma-interferon induced programmed cell death
8	EMP1	−24.18	AC079628	Play an important role in cell growth, cell proliferation, epidermis development and multicellular organismal development
9	ZMAT3	−24.17	XM_002912444	May play role in the TP53-dependent growth regulatory pathway
10	UBE2J1	−22.88	NM_019586	Catalyzes the covalent attachment of ubiquitin to other proteins
11	UBE2G1	−18	NM_022690	Accepts ubiquitin from the E1 complex and catalyzes its covalent attachment to other protein
12	THRAP3	−17.14	XM_535012	Involved in pre-mRNA splicing
13	HDAC7	−16.6	AC004466	Transcription regulation, cell cycle progression, and developmental events
14	PDCD2	−13.27	XM_002817611	Cell death and/or in regulation of cell proliferation

FDR false discovery rate <0.05; *PFC* proportion fold change

Table 7 List of up-regulated genes from apoptosis cluster

	Genes	PFC	Accession no.	Function
1	BATF2	∞	XM_850420	Control differentiation of lineage-specific cells in the immune system
2	PDCD5	∞	DQ023265	Regulator of K acetyltranferase 5 that involved in transcription, DNA damage response and cell cycle control
3	RASSF1	∞	XM_001495988	Tumour suppressor as it is required for receptor-dependent apoptosis
4	LOXL1	∞	NM_010729	Essential to the biogenesis of connective tissue, encoding an extracellular copper-dependent amine oxide
5	CBX1	∞	XM_002928442	Recognize and binds Histone H3 tails methylated at 'Lys-9′, leading to epigenetic repression
6	UBE2S	∞	XM_541410	Form a thiol ester linkage with ubiquitin
7	XRCC1	∞	NM_053435	Repair single strand breaks in DNA
8	NFKBIA	17.63	XM_003410238	Inhibit NF-kappa-B/REL complexes
9	TRAF2	13.09	XM_852196	Play an important role in cell survival and apoptosis
10	FASTK	12.55	XM_002915491	Phosphorylates the splicing regulator TIA1
11	SOLH	11.93	XM_547218	May function as transcription factor, RNA-binding protein, or in protein–protein interactions during visual system development
12	MAGEB16	10.79	CU457723	Melanoma-associated antigen B16
13	IFNAR2	9.78	XM_544861	Associates with IFNAR1 to form type 1 interferon receptor
14	LGALS3BP	8.71	HQ637390	Modulating cell–cell and cell–matrix interaction

FDR false discovery rate <0.05; *PFC* proportion fold change

induced TNFR1 signaling pathways and caused both apoptosis and TNF mediated NF-kB activation [25, 26]. FADD protein also contains a death domain that act as a bridge between Fas receptors and different procaspases, which form the death-induction signaling complex (DISC) during apoptosis [27]. In addition to FADD, DAXX was also unregulated. The C-terminal of this protein can interact with FADD and also activate Jun N-terminal kinase (JNK) and apoptosis pathways [28]. Hence, TNF- α play a pivotal role in apoptosis during FIPV infection, and

Table 8 Apoptosis signaling pathway genes that affected by FIPV

	Genes	PFC	Role in apoptosis signaling pathway
1	ATF7	−48.46	Activating transcription factor
2	TMBIM6	−4.99	Bax inhibitor-1
3	PRKCD	−2.51	Protein kinase C
4	CASP7	−4.80	Caspase 7
5	MAP4K5	−2.95	Germinal center kinase related
6	CHUK	−8.23	Inhibitor of kappa-B kinase
7	HSPA8	−122.90	Heat shock protein 70
8	FOSL2	−10.30	Activating transcription factor
9	MAPK8	−2.73	Jun kinase
10	AKT3	−3.65	Protein kinase B
11	PRKCA	−7.37	Protein kinase C
12	MAPK3	−2.36	Mitogen activated protein kinase
13	MAPK9	−10.82	Jun kinase
14	MAPK1	−15.80	Mitogen activated protein kinase
15	ATF1	−2.59	Activating transcription factor
16	ATF4	3.57	Activating transcription factor
17	DAXX	5.63	Death-associated protein 6
18	ENDOG	4.41	Endonuclease G
19	HSPA2	3.18	Heat shock protein 70
20	TRAF2	13.90	TNF receptor-associated factor 2
21	NFKBIB	6.39	Inhibitor of kappa light chain gene enhancer in B cells
22	TRADD	6.49	TNFR1 associated death domain
23	NFKB2	4.78	Nuclear factor kappa-B
24	NFKBIA	17.63	Inhibitor of kappa light chain gene enhancer in B cells
25	FADD	2.37	Fas associated death domain

FDR false discovery rate <0.05; *PFC* proportion fold change

according to our results, both mRNA and protein levels of this cytokine were significantly increased in the first 3 hpi, which would affect many of aforementioned pathways that induce apoptosis.

After investigation of the trend of apoptosis and expression change of selected genes from apoptosis cluster, the TNF receptor-associated factor 2 (TRAF2) and programmed cell death-5 (PDCD5) were the only genes that showed significant up regulation from the first hour after infection (Fig. 3). Hence, the process of apoptosis induction of FIPV would be started as early as 1 hpi. However this process could not be detected by flow cytometry until 9 hpi. PDCD5 is a pro-apoptotic gene that is highly expressed in cells that undergo apoptosis [29] and may participate in the pathophysiologic course of disease involving abnormal programmed cell death [30]. Previous study also has showed that FIPV can up regulate the expression of programmed cell death-1 (PDCD1), a known pro apoptotic gene after 3 hpi [22].

On the other hand, an anti-apoptotic gene like TRAF2 would be up regulated after 1 hpi. This gene is involved in apoptosis signaling and p53 pathways, which plays an important role in protecting cells from ER stress induced apoptosis [31]. Therefore, these two pathways would be affected from the first hour of infection. It is shown that TRAF2 depletion lowers the signal threshold for death receptor-mediated apoptosis [32]. The delicate balance between pro- and anti-apoptotic molecules during coronavirus (CoV) infection enables rapid multiplication of virus before cell lysis [33]. It has been shown that anti-apoptotic response induced by SARS CoV infection in infected enterocytes is important to inhibit or delay cell destruction, which results in extending virus production and shedding. The SARS CoV has a protein named ORF 3a that shows high pro-apoptotic properties through the cell receptors and mitochondrial pathways [34]. Similarly, FIPV has a mutant of this protein that named ORF 3c with high expression in the death tissues of the infected cats [6]. However, the direct involvement of this gene in FIPV induced apoptosis of the infected cells has not been studied.

After 9 hpi, two other pro apoptotic genes, Ras Association Domain-Containing Protein-1 (RASSF1) and basic leucine zipper transcriptional factor ATF-like 2 (BATF2), also showed up regulation. Hence, it can be concluded that

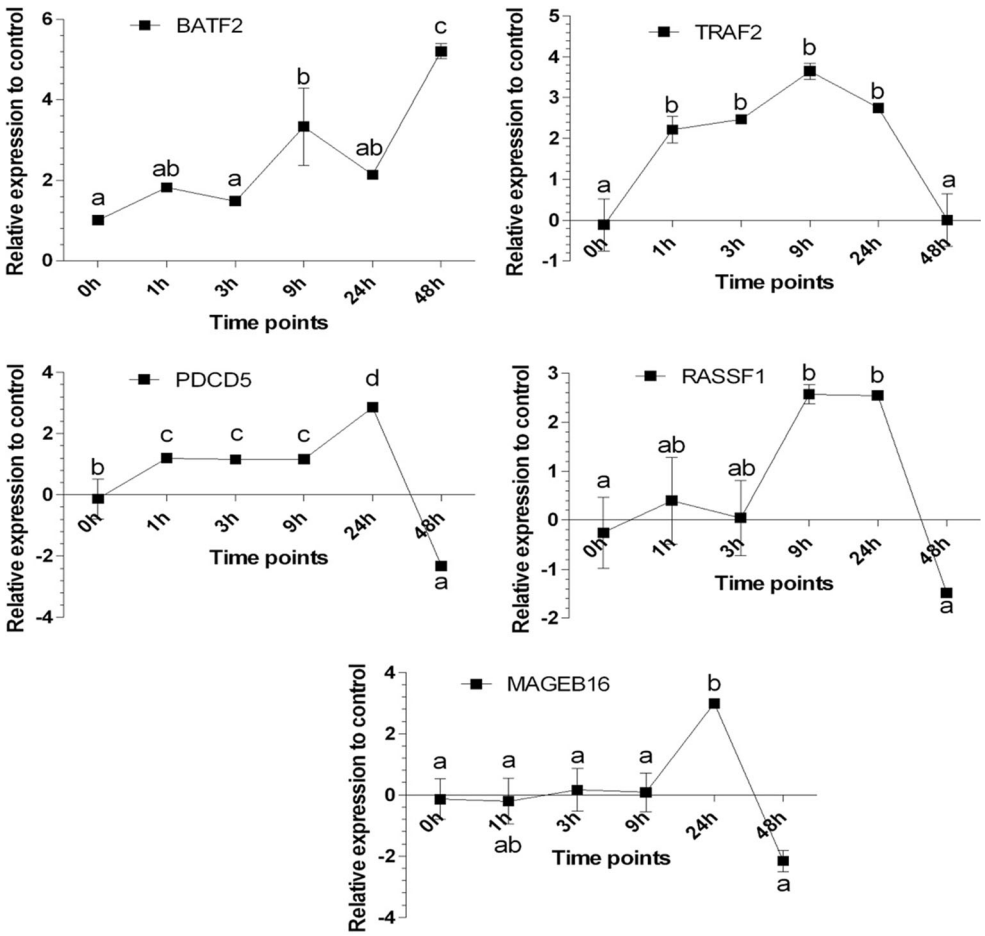

Fig. 4 Relative expression of selected genes to their control (ΔΔCq) with RT-qPCR. The alphabets on the figures show the post hoc Turkey HSD results of the differences amongst the time points at 0.05 level of significance

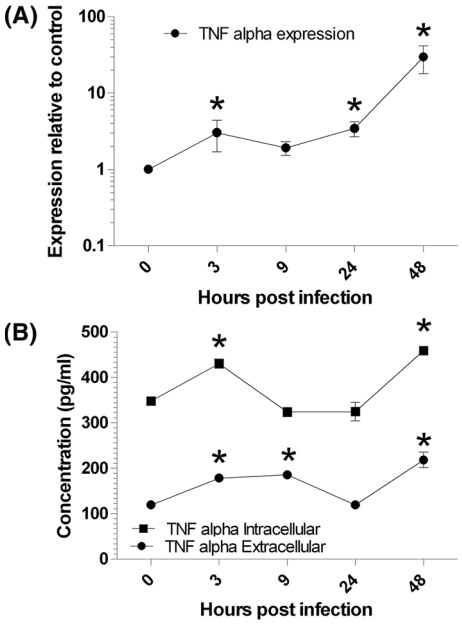

Fig. 5 mRNA expression (**a**) and protein concentration (**b**) changes of TNFα in first 48 h of FIPV infection in CRFK cells

increase of communalities of pro apoptotic genes at this time point lead to significant augmentation of the number of early apoptosis cells and depletion of the viable cells. RASSF1 is known as a tumor suppressor gene by inducing cell cycle arrest at G(1)/S phase of cell cycle progression [35]. This gene can serve as a novel Ras effector [36], and enhance apoptosis [37]. Over expression of BATF2 or SARI (AP1-protein suppressor), another gene of interest of current study, can result in inhibition of DNA binding activation protein (AP1), which causes growth inhibition and induced apoptosis particularly in cancerous cells [38]. Hence, AP1 protein and IFN-β can be another factors involved in FIPV apoptosis induction. The results of this study also showed significant (FDR <0.05) up regulation in IFN α/β receptor 2 and down regulation of AP1 complex subunit beta-1 (AP1B1), which confirms the mechanism of action of BATF2 in apoptosis induction. Down regulation of BATF2 may result in poor prognosis of different types of carcinoma like hepato-cellular and squamous cell carcinoma [39, 40]. This gene is also up regulated in some other viral diseases like hepatitis E and hepatitis C [41, 42].

Significant increase in the number of necrosis cells was detected starting at 24 hpi (Figs. 1 and 2; Table 2). All the selected genes showed high up regulations in this time point. Melanoma-associated antigen B16 (MAGEB16) also started to up regulate at this time point. The MAGE genes have come under attention of many scientists for gene therapy in cancer and even viral diseases [43, 44]. Different MAGE genes play variety of roles in apoptosis and cell activities [44]. The activation of these genes make them the antigenic targets for immune system [44]. For instance, co expression of MAGED1 and P75NTR of the neutrophils will result in enhancement of cellular apoptosis [43]. Hence, MAGEB16 can play an important role in late stages of apoptosis and necrosis of the cells during FIPV infection. After 48 hpi, BATF2 still showed high up regulation. Hence, this gene is an important factor during death stages of the cells. In this time point, all the other selected genes, even an anti apoptotic gene like TRAF2 were down regulated. Hence, it can be concluded that other mechanisms and pathways are involved in this stage.

In conclusion, transcriptome analysis can be a promising approach in understanding the pathogenesis and underlying factors involved in pathogenesis of FCoVs or other viruses. This study managed to propose the onset time of early and late apoptosis in FIPV infection and also identified the factors and pathways involved during FIPV infection. More studies are required to understand the role of these genes from different cellular functions, molecular processes, and biological pathways during FIPV pathogenesis. Among variety of involved factors, we have underlined the importance of apoptosis during FIPV infection.

Acknowledgments This work was supported by Grant Number 01-11-08-6390FR from Ministry of Education, Malaysia. The funder had no role in the study design, data collection and analysis, or preparation of the manuscript.

Authors' Contributions ANS, NS, MSRH and ARO co-defined the research theme. ANS, NS, MSRH and ARO designed the experiments. ANS, NS, AH, MSRH, SWT carried out the laboratory experiments. AH, NS, PM and ARO analyzed and interpreted the data. AH, NS and ARO had written the manuscript. All authors revised the manuscript thoroughly and approved the final manuscript.

Compliance with Ethical Standards

Conflict of interest The authors have declared that no conflict of interest exists.

References

1. Simons FA, Vennema H, Rofina JE, Pol JM, Horzinek MC, Rottier PJ, Egberink HF (2005) A mRNA PCR for the diagnosis of feline infectious peritonitis. J Virol Methods 124(1–2): 111–116. doi:10.1016/j.jviromet.2004.11.012
2. Vennema H, Poland A, Foley J, Pedersen NC (1998) Feline infectious peritonitis viruses arise by mutation from endemic feline enteric coronaviruses. Virology 243(1):150–157. doi:10.1006/viro.1998.9045
3. Kipar A, Meli ML (2014) Feline infectious peritonitis: still an enigma? Vet Pathol 51(2):505–526. doi:10.1177/0300985814522077
4. Kipar A, Meli ML, Baptiste KE, Bowker LJ, Lutz H (2010) Sites of feline coronavirus persistence in healthy cats. J Gen Virol 91(Pt 7):1698–1707. doi:10.1099/vir.0.020214-0
5. Pedersen NC (2014) An update on feline infectious peritonitis: virology and immunopathogenesis. Vet J 201(2):123–132. doi:10.1016/j.tvjl.2014.04.017
6. Pedersen NC (2009) A review of feline infectious peritonitis virus infection: 1963-2008. J Feline Med Surg 11(4):225–258. doi:10.1016/j.jfms.2008.09.008
7. Amer A, Siti Suri A, Abdul Rahman O, Mohd HB, Faruku B, Saeed S, Tengku Azmi TI (2012) Isolation and molecular characterization of type I and type II feline coronavirus in Malaysia. Virol J 9(1):278. doi:10.1186/1743-422X-9-278
8. An DJ, Jeoung HY, Jeong W, Park JY, Lee MH, Park BK (2011) Prevalence of Korean cats with natural feline coronavirus infections. Virol J 8(1):455. doi:10.1186/1743-422X-8-455
9. Petersen NC, Boyle JF (1980) Immunologic phenomena in the effusive form of feline infectious peritonitis. Am J Vet Res 41(6):868–876
10. Takano T, Hohdatsu T, Hashida Y, Kaneko Y, Tanabe M, Koyama H (2007) A "possible" involvement of TNF-alpha in apoptosis induction in peripheral blood lymphocytes of cats with feline infectious peritonitis. Vet Microbiol 119(2–4):121–131. doi:10.1016/j.vetmic.2006.08.033
11. Gelain ME, Meli M, Paltrinieri S (2006) Whole blood cytokine profiles in cats infected by feline coronavirus and healthy non-FCoV infected specific pathogen-free cats. J Feline Med Surg 8(6):389–399. doi:10.1016/j.jfms.2006.05.002
12. Mortazavi A, Williams BA, McCue K, Schaeffer L, Wold B (2008) Mapping and quantifying mammalian transcriptomes by RNA-Seq. Nat Methods 5(7):621–628. doi:10.1038/nmeth.1226
13. Thomas PD, Campbell MJ, Kejariwal A, Mi H, Karlak B, Daverman R, Diemer K, Muruganujan A, Narechania A (2003) PANTHER: a library of protein families and subfamilies indexed by function. Genome Res 13(9):2129–2141. doi:10.1101/gr.772403
14. Mizuno T, Momoi Y, Endo Y, Nishimura Y, Goto Y, Ohno K, Watari T, Tsujimoto H, Hasegawa A (1997) Apoptosis enhanced by soluble factor produced in feline immunodeficiency virus infection. J Vet Med Sci 59(11):1049–1051. doi:10.1292/jvms.59.1049
15. Van Hamme E, Dewerchin HL, Cornelissen E, Verhasselt B, Nauwynck HJ (2008) Clathrin- and caveolae-independent entry of feline infectious peritonitis virus in monocytes depends on dynamin. J Gen Virol 89(Pt 9):2147–2156. doi:10.1099/vir.0.2008/001602-0
16. Stoddart CA, Scott FW (1989) Intrinsic resistance of feline peritoneal macrophages to coronavirus infection correlates with in vivo virulence. J Virol 63(1):436–440
17. Li X, Scott FW (1994) Detection of feline coronaviruses in cell cultures and in fresh and fixed feline tissues using polymerase chain reaction. Vet Microbiol 42(1):65–77. doi:10.1016/0378-1135(94)90078-7
18. Mizuno T, Goto Y, Baba K, Masuda K, Ohno K, Tsujimoto H (2001) TNF-alpha-induced cell death in feline immunodeficiency virus-infected cells is mediated by the caspase cascade. Virology 287(2):446–455. doi:10.1006/viro.2001.1042
19. Natoni A, Kass GE, Carter MJ, Roberts LO (2006) The mitochondrial pathway of apoptosis is triggered during feline

calicivirus infection. J Gen Virol 87(Pt 2):357–361. doi:10.1099/vir.0.81399-0
20. Haagmans BL, Egberink HF, Horzinek MC (1996) Apoptosis and T-cell depletion during feline infectious peritonitis. J Virol 70(12):8977–8983
21. Takano T, Azuma N, Hashida Y, Satoh R, Hohdatsu T (2009) B-cell activation in cats with feline infectious peritonitis (FIP) by FIP-virus-induced B-cell differentiation/survival factors. Arch Virol 154(1):27–35. doi:10.1007/s00705-008-0265-9
22. Harun MS, Kuan CO, Selvarajah GT, Wei TS, Arshad SS, Hair Bejo M, Omar AR (2013) Transcriptional profiling of feline infectious peritonitis virus infection in CRFK cells and in PBMCs from FIP diagnosed cats. Virol J 10(1):329. doi:10.1186/1743-422X-10-329
23. Takano T, Ohyama T, Kokumoto A, Satoh R, Hohdatsu T (2011) Vascular endothelial growth factor (VEGF), produced by feline infectious peritonitis (FIP) virus-infected monocytes and macrophages, induces vascular permeability and effusion in cats with FIP. Virus Res 158(1–2):161–168. doi:10.1016/j.virusres.2011.03.027
24. Regan AD, Cohen RD, Whittaker GR (2009) Activation of p38 MAPK by feline infectious peritonitis virus regulates pro-inflammatory cytokine production in primary blood-derived feline mononuclear cells. Virology 384(1):135–143. doi:10.1016/j.virol.2008.11.006
25. Hsu H, Shu HB, Pan MG, Goeddel DV (1996) TRADD-TRAF2 and TRADD-FADD interactions define two distinct TNF receptor 1 signal transduction pathways. Cell 84(2):299–308. doi:10.1016/S0092-8674(00)80984-8
26. Hsu H (1995) The TNF receptor 1-associated protein TRADD signals cell death and NF-κB activation. Cell 81(4):495–504. doi:10.1016/0092-8674(95)90070-5
27. Kischkel FC, Hellbardt S, Behrmann I, Germer M, Pawlita M, Krammer PH, Peter ME (1995) Cytotoxicity-dependent APO-1 (Fas/CD95)-associated proteins form a death-inducing signaling complex (DISC) with the receptor. EMBO J 14(22):5579–5588
28. Yang X, Khosravi-Far R, Chang HY, Baltimore D (1997) Daxx, a novel Fas-binding protein that activates JNK and apoptosis. Cell 89(7):1067–1076. doi:10.1016/s0092-8674(00)80294-9
29. Chen Y, Sun R, Han W, Zhang Y, Song Q, Di C, Ma D (2001) Nuclear translocation of PDCD5 (TFAR19): an early signal for apoptosis? FEBS Lett 509(2):191–196. doi:10.1016/S0014-5793(01)03062-9
30. Yao H, Xu L, Feng Y, Liu D, Chen Y, Wang J (2009) Structure-function correlation of human programmed cell death 5 protein. Arch Biochem Biophys 486(2):141–149. doi:10.1016/j.abb.2009.03.018
31. Mauro C, Crescenzi E, De Mattia R, Pacifico F, Mellone S, Salzano S, de Luca C, D'Adamio L, Palumbo G, Formisano S, Vito P, Leonardi A (2006) Central role of the scaffold protein tumor necrosis factor receptor-associated factor 2 in regulating endoplasmic reticulum stress-induced apoptosis. J Biol Chem 281(5):2631–2638. doi:10.1074/jbc.M502181200
32. Gonzalvez F, Lawrence D, Yang B, Yee S, Pitti R, Marsters S, Pham VC, Stephan JP, Lill J, Ashkenazi A (2012) TRAF2 sets a threshold for extrinsic apoptosis by tagging caspase-8 with a ubiquitin shutoff timer. Mol Cell 48(6):888–899. doi:10.1016/j.molcel.2012.09.031
33. Enjuanes L, Almazan F, Sola I, Zuniga S (2006) Biochemical aspects of coronavirus replication and virus-host interaction. Annu Rev Microbiol 60:211–230. doi:10.1146/annurev.micro.60.080805.142157
34. McBride R, Fielding BC (2012) The role of severe acute respiratory syndrome (SARS)-coronavirus accessory proteins in virus pathogenesis. Viruses 4(11):2902–2923. doi:10.3390/v4112902
35. Shivakumar L, Minna J, Sakamaki T, Pestell R, White MA (2002) The RASSF1A tumor suppressor blocks cell cycle progression and inhibits cyclin D1 accumulation. Mol Cell Biol 22(12):4309–4318. doi:10.1128/MCB.22.12.4309-4318.2002
36. Vos MD, Ellis CA, Bell A, Birrer MJ, Clark GJ (2000) Ras uses the novel tumor suppressor RASSF1 as an effector to mediate apoptosis. J Biol Chem 275(46):35669–35672. doi:10.1074/jbc.C000463200
37. Cox AD, Der CJ (2003) The dark side of Ras: regulation of apoptosis. Oncogene 22(56):8999–9006. doi:10.1038/sj.onc.1207111
38. Su ZZ, Lee SG, Emdad L, Lebdeva IV, Gupta P, Valerie K, Sarkar D, Fisher PB (2008) Cloning and characterization of SARI (suppressor of AP-1, regulated by IFN). Proc Natl Acad Sci USA 105(52):20906–20911. doi:10.1073/pnas.0807975106
39. Ma H, Liang X, Chen Y, Pan K, Sun J, Wang H, Wang Q, Li Y, Zhao J, Li J, Chen M, Xia J (2011) Decreased expression of BATF2 is associated with a poor prognosis in hepatocellular carcinoma. Int J Cancer 128(4):771–777. doi:10.1002/ijc.25407
40. Wen H, Chen Y, Hu Z, Mo Q, Tang J, Sun C (2014) Decreased expression of BATF2 is significantly associated with poor prognosis in oral tongue squamous cell carcinoma. Oncol Rep 31(1):169–174. doi:10.3892/or.2013.2863
41. Moal V, Textoris J, Ben Amara A, Mehraj V, Berland Y, Colson P, Mege JL (2013) Chronic hepatitis E virus infection is specifically associated with an interferon-related transcriptional program. J Infect Dis 207(1):125–132. doi:10.1093/infdis/jis632
42. Yu C, Boon D, McDonald SL, Myers TG, Tomioka K, Nguyen H, Engle RE, Govindarajan S, Emerson SU, Purcell RH (2010) Pathogenesis of hepatitis E virus and hepatitis C virus in chimpanzees: similarities and differences. J Virol 84(21):11264–11278. doi:10.1128/JVI.01205-10
43. Barker PA, Salehi A (2002) The MAGE proteins: emerging roles in cell cycle progression, apoptosis, and neurogenetic disease. J Neurosci Res 67(6):705–712. doi:10.1002/jnr.10160
44. Xiao J, Chen HS (2004) Biological functions of melanoma-associated antigens. World J Gastroenterol 10(13):1849–1853